

# Vibration Damping With Urethane/Acrylate Simultaneous Semi-Interpenetrating Polymer Networks

CHEIN-JEN TUNG and TZU-CHIEN J. HSU\*

Institute of Materials Science and Engineering, National Sun Yat-Sen University,  
Kaohsiung 804, Taiwan, Republic of China

## SYNOPSIS

The vibration damping efficiency of the IPN-laminated steel sheet, which consisted of a viscoelastic IPN layer sandwiched between two steel sheets, was investigated in this study. The simultaneous semi-IPN used included an elastomeric urethane phase and a glassy acrylate phase. This study seeks to develop a laminate, with broader damping temperature and frequency ranges, in contrast to the homopolymer-based laminates studied previously. A vibration damping analysis of the neat IPNs was first conducted using a dynamic rheometer in order to provide basic rheological properties of the neat IPNs. This was followed by the frequency spectrum analysis of the IPN-based laminates, using a frequency analyzer, utilizing the results derived from the damping analysis of the neat IPNs. The IPN variables studied included the reaction temperature, the amount of the catalyst for urethane phase, the composition in acrylate phase and in urethane phase, and the composition of IPN. The results indicated that, by properly adjusting the IPN parameters, the extent of phase separation in IPN could be controlled. The effect of the network formation in the catalyzed urethane phase on the damping properties of IPNs was also investigated and the possible reaction mechanism was analyzed. The IPNs with catalyzed urethane phase showed single, smooth damping curves with peak values of  $\tan \delta = 0.4\text{--}0.7$  in a broad temperature range. The study was then extended to the analysis of the vibration damping efficiency of the IPN-based laminates, including the effect of IPN composition, the effect of the urethane composition in IPN, and the effect of the acrylate composition in IPN. The results indicated that the IPN-based laminates yielded a maximum loss factor in the range of 0.1–0.5, which was below the  $\tan \delta$  value of IPN, but was better than that of the neat steel sheet. In addition, most of the damping properties of the laminates could be derived or predicted from the dynamic rheological properties of the neat IPNs. Thus, knowing the basic dynamic rheological properties of the neat IPNs is vital for a successful design and application of the IPN-laminated steel sheet. © 1992 John Wiley & Sons, Inc.

## INTRODUCTION

The use of viscoelastic polymer as a vibration damping material is becoming increasingly important for noise reduction and, in some applications, fatigue failure prevention. Examples include its applications in the aerospace industry, the automobile industry, the building industry, and house appliance industry.<sup>1–5</sup> The polymer-laminated steel sheet is one of the successful applications and has been com-

mercialized in recent years.<sup>6,7</sup> The laminate, schematically illustrated in Figure 1, usually consists of a polymeric layer that is sandwiched between two steel sheets. The constrained polymeric layer provides shear deformation, which can convert mechanical energy into heat. The noise is thus considerably reduced. The mechanism of this conversion is primarily due to the local segmental motion in the polymer chain occurring at the glass transition temperature, and the intermolecular friction by the relative motion of main back bone chains. Another type of damping, called the extensional damping, utilizes primarily the extensional and flexural motions of the polymer molecules.

\* To whom correspondence should be addressed.

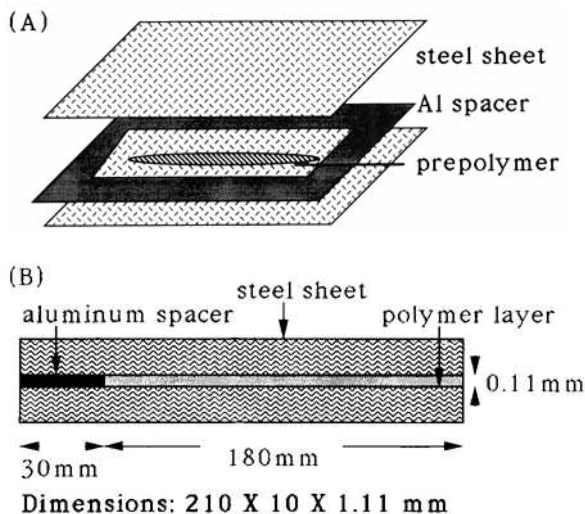


**Figure 1** Basic configuration of the IPN-laminated steel sheet (A) and the dimensions of the laminate used for frequency spectrum analysis (B).

In the previous study in this laboratory,<sup>4</sup> efforts have been concentrated on the use of homopolymers to develop a room-temperature type and a high-temperature type laminate. A poly(vinyl butyral) and a polymer consisting of ethylene and acrylic acid were selected because of their excellent vibration damping properties and good adhesive strength with steel sheet. A theoretical damping analysis, based on a model proposed by Ross, Ungar, and Kerwin (the RUK approach), was also applied in order to provide fundamental understanding of the damping mechanism and the variables affecting the damping efficiency of the laminate.<sup>5,8-10</sup>

Generally speaking, the acoustic frequency of practical interest is in the range of 20 Hz to 20,000 Hz. In order to apply successfully the model proposed by RUK to the polymer-laminated steel sheet, one needs to obtain the rheological data at the required frequency range. However, measurement of storage modulus and tangent delta on any commercially available rheometer (such as the RDA series from Rheometrics and others) is limited to a narrow frequency range, that is, only up to approximately 100 Hz. To meet this requirement, Liao and Hsu<sup>11</sup> applied the time-temperature superposition principle to the two polymers mentioned above in order to obtain high frequency rheological data from low temperature measurement. Although a discrepancy existed between the experimentally measured data and the loss factors of the laminate predicted with superposed and without superposed data, a detailed analysis was given in their work.

However, the useful damping temperature range of a homopolymer usually covers 20–30°C for acoustical frequency ranging from 20 Hz to 20,000 Hz.<sup>2</sup> To meet the requirement of various vibrating systems, which could require a broader damping temperature and frequency ranges, it was necessary to develop a polymer that possessed a broad glass transition range. An effective way to develop this is to combine two or more polymers, which are mixed at the molecular level, to yield a broader glass transition range. This necessitates the use of interpenetrating polymer networks (IPNs).

The term IPN denotes an entirely new class of material. An IPN is a polymer alloy of two polymers, which have been synthesized or crosslinked in the presence of each other.<sup>12,13</sup> An IPN is characterized by low enthalpy and high entropy of mixing of monomer and monomer (simultaneous IPN) or of monomer and polymer (sequential IPN), rather than of polymer and polymer (polymer blend).

In this work, a simultaneous semi-IPN, consisting of an elastomeric urethane phase and a glassy acrylate phase, was used. The urethane phase was chosen due to its elastomeric property and excellent damping capability. The acrylate phase was chosen mainly because of its high damping and good adhesive strength with the steel sheet. A great deal of research has been concentrated on the studies of urethane/acrylate IPNs, including studies of their synthesis, morphology, and mechanical properties, but seldom on their damping efficiency,<sup>14-18</sup> nor on the IPN-laminated steel sheet.

In recent years, there has been increasing interest in polymers for vibration and damping applications. Most of the research has concentrated on the damping properties of neat polymers, polymer foams,<sup>19</sup> and IPNs.<sup>18,20</sup> The effect of fillers on the damping properties of urethane/epoxy IPNs has also been addressed.<sup>21</sup> Fay et al. proposed that the area under the linear loss modulus-temperature curve, measured from dynamic mechanical spectroscopy, could be related to the chemical composition of the polymer used and damping capability could be quantified from the loss area.<sup>22</sup> However, research has seldom been directed towards the evaluation of the damping efficiency of the IPN-laminated steel sheet.

Preparation of the simultaneous IPN is an example of reactive polymer processing, which can be characterized as (1) bulk state, (2) fast reaction, (3) high exotherm, and (4) short cycle time. In reactive processing of simultaneous IPNs, the chemical reaction is further complicated by the physical changes, including gelation, crystallization, glass transition, phase separation, and network formation.

**Table I** Ingredients of IPN Used and Sample Designation

Sample Code	U/A (by wt)	Urethane (U) (Polyol/MDI) (by eq) (by wt)	Acrylate (A) (MMA/MA) (by wt)	Cat. in U (wt %)	Curing Temp. (°C)
P-10	1/0	1/1.04 (1.9/1)	—	—	80
P-01	0/1	—	1/1	—	65
P-02	0/1	—	1/0	—	65
P-11	2/1	1/1.04 (1.9/1)	1/1	—	70
P-11c	2/1	1/1.04 (1.9/1)	1/1	0.01	70
P-12	2/1	1/104 (1.9/1)	1/0	—	80
P-12c	2/1	1/1.04 (1.9/1)	1/0	0.01	45
P-12	1/1	1/1.04 (1.9/1)	1/0	—	80
P-12c	1/1	1/1.04 (1.9/1)	1/0	0.01	35
P-13c	2/1	1/1.02 (1.9/1)	0/1	0.01	70 <sup>a</sup>
P-23c	2/1	1/1.04 (1.3/1)	0/1	0.01	70 <sup>a</sup>
P-33c	2/1	1/1.05 (5.3/1)	0/1	0.01	70 <sup>a</sup>

<sup>a</sup> The press temperature for the preparation of laminates.

These physical changes occur during the reaction and interact with the reaction and thus affect the properties of the finished polymers.

In this study, the vibration damping analysis of IPNs is first conducted in order to provide detailed dynamic rheological properties of the IPNs. This is followed by the frequency spectrum analysis of the IPN-laminated steel sheet in order to obtain the loss factor of the laminate, utilizing the results derived from the vibration damping analysis of IPNs.

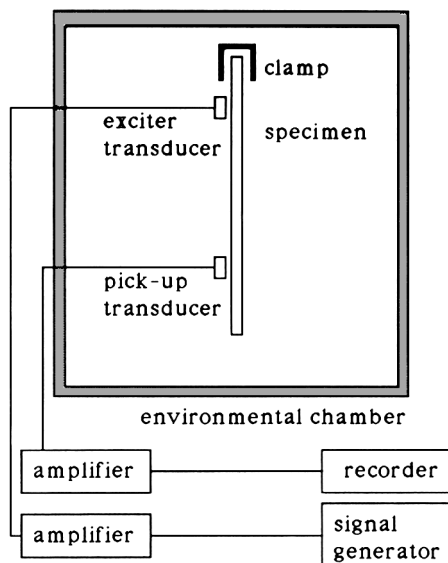


**Figure 2** Schematic diagram illustrating the frequency spectrum analysis.

## EXPERIMENTAL

### Materials

The basic structure of the IPN-laminated steel sheet used in this study included two 0.50-mm-thick steel sheets, laminated with a viscoelastic polymer film of 0.11 mm in thickness (Fig. 1). The raw steel sheet was a cold-rolled steel sheet (SPCC, China Steel Corp.) and no surface treatment was applied. The ingredients of the simultaneous semi-IPNs, listed in Table I, consisted of an elastomeric urethane phase and a glassy acrylate phase (urethane/acrylate IPN). The urethane phase (thermoset) included a diol (A 1003, MW = 200 g/eq), a triol (A 1455,

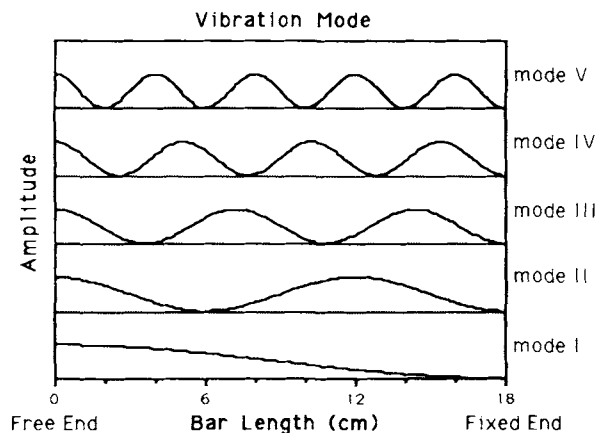


**Figure 3** Vibration modes of IPN-based laminates detected in the frequency spectrum analysis.

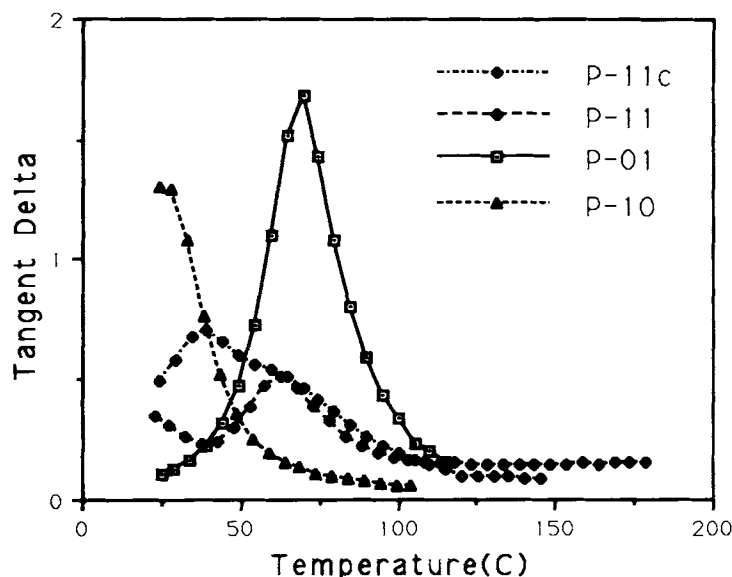


Figure 4 Plots of tangent delta vs. temperature of P-11 series and their components.

MW = 1000 g/eq)—both were based on polyether polyol and were supplied by Chiunglong Chemicals Co.—and a modified diphenyl methane diisocyanate MDI (Millionate MTLC, NCO content = 28.5%, MW = 143.4 g/eq, from Mitsubishi Petrochemical Co.). All of the ingredients of urethane phase were used as received. Di-butyltin dilaurate (T-12, M&T Chemicals) was used as catalyst at a level of 0.01 wt %. The acrylate phase (thermoplastic) included methyl methacrylate (MMA), methyl acrylate (MA), and a random copolymer of MMA and MA (MMA/MA); all were supplied by Eternal Chemical Co. (Taiwan), and were used as received. The initiator for all the acrylates was AIBN, with 1.0 wt %.

### Sample Designation

Sample designation of IPNs and its components is explained as follows: The letter *P* refers to the neat IPN used, whereas the letter *L* refers to the IPN-laminated steel sheet (the laminate). The first number, from 1–3, indicates the different type of the urethane phase used, while the second number, also from 1–3, indicates the different type of the acrylate phase. The number 0 implies nothing was presented in the indicated phase. Finally, the last letter *c* indicates that the urethane phase was catalyzed using T-12.

Sample designation of the IPN-laminated steel sheet is all the same as that of neat IPN, except the first letter is changed from *P* to *L*. Since the urethane phase in all the IPNs laminated with steel sheet were catalyzed using T-12, the last *c* is omitted

for simplicity in the designation of the IPN-based laminates.

### Sample Preparation and Instrumentation

#### Dynamic Mechanical Analysis

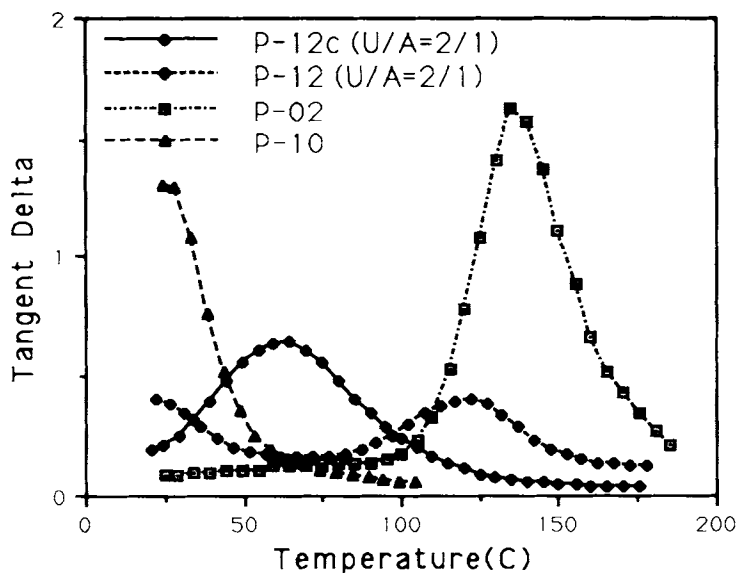
For polyacrylates, polyurethanes, and their IPNs, the components of them were sealed with nitrogen gas in a 50 cc polypropylene bottle. After thorough mixing by vigorous shaking, the mixture was allowed to polymerize in an oven at a specified temperature.

Table II Tan  $\delta$  Peak Value, Peak Temperature, and Peak Temperature Range of IPNs and Their Components

Sample Code	Tan $\delta$ Peak Value		Tan $\delta$ Peak Temp. ( $^{\circ}$ C)		$\Delta T^a$ ( $^{\circ}$ C)
	1st	2nd	1st	2nd	
P-10	11.3	—	< 25	—	30
P-01	—	1.7	—	75	50
P-02	—	1.63	—	135	5
P-11	< 0.4	0.51	< 25	63	11
P-11c	0.7 (0.54) <sup>b</sup>	—	39 (60) <sup>b</sup>	—	55
P-12	< 0.5	0.41	< 20	122	5
P-12c	—	0.64	—	64	50
P-12	< 0.22	0.73	< 25	121	31
P-12c	—	0.46 (0.31) <sup>b</sup>	—	116 (70) <sup>b</sup>	32

<sup>a</sup> Temperature range in which all tan  $\delta$  greater than 0.4.

<sup>b</sup> The number in parentheses indicates that the peak is only a shoulder.



**Figure 5** Plots of tangent delta vs. temperature of P-12 ( $U/A = 2/1$ ) series and their components.

The storage modulus and the tangent delta of the polymer samples were measured using a dynamic rheometer (RDA-II, Rheometrics). Sample dimensions for RDA experiment were about  $38.0 \times 12.5 \times 3.25$  mm. All the samples were run twice in RDA in the same manner, the second run data were taken. The frequency for all tests was set at 10 Hz (62.8 rad/sec).

#### Frequency Spectrum Analysis

Preparation of the sandwich-type laminated steel sheet is illustrated in Figure 1. The prepolymer was prepared by polymerizing the mixed monomers to a viscosity of about 10 poises. The prepolymer was then coated to one steel sheet, putting on an aluminum spacer and the other steel sheet on the top

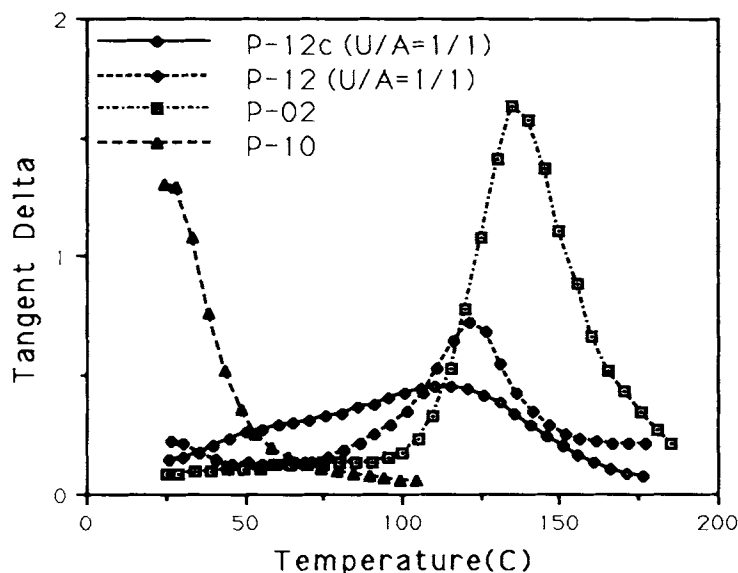


**Figure 6** Plots of tangent delta vs. temperature of P-12 ( $U/A = 1/1$ ) series and their components.

as the constraining layer; it was then allowed to polymerize for 4 h in a thermal press (Model MTP-14, Tetrahedron Assoc., Inc.) The press temperature was controlled at 70°C for all laminates. Press pressure was controlled at 44 atm in order to obtain a constant and uniform thickness of the viscoelastic film. After curing, the laminate was further post-cured at 150°C for 15 min. Figure 1 (B) shows the dimensions of the IPN-laminated steel sheet.

Shown in Figure 2 is the schematic diagram, illustrating the experimental set-up for the vibration test. Before testing, the laminates were thermally aged for 3 h at a temperature 10°C above the glass transition temperature of the laminated IPN. This

eliminated any possible residual thermal stress in the laminate. During testing, a random noise excitation was sent to the specimen via a magnetic transducer (Type MM0002, B & K Co., Denmark) to force the laminate to vibrate. The response was detected by a capacitive transducer (Type MM0004). Both input and output signals were fed into a fast Fourier transform signal analyzer (Type 2032) and then were analyzed in the frequency range of 0 to 1600 Hz with the Hanning window function. The frequency spectra were continuously recorded during the test. Zoom analysis was also performed to improve the resolution and the accuracy of the spectrum. The loss factor of the laminate,  $\eta$ , was

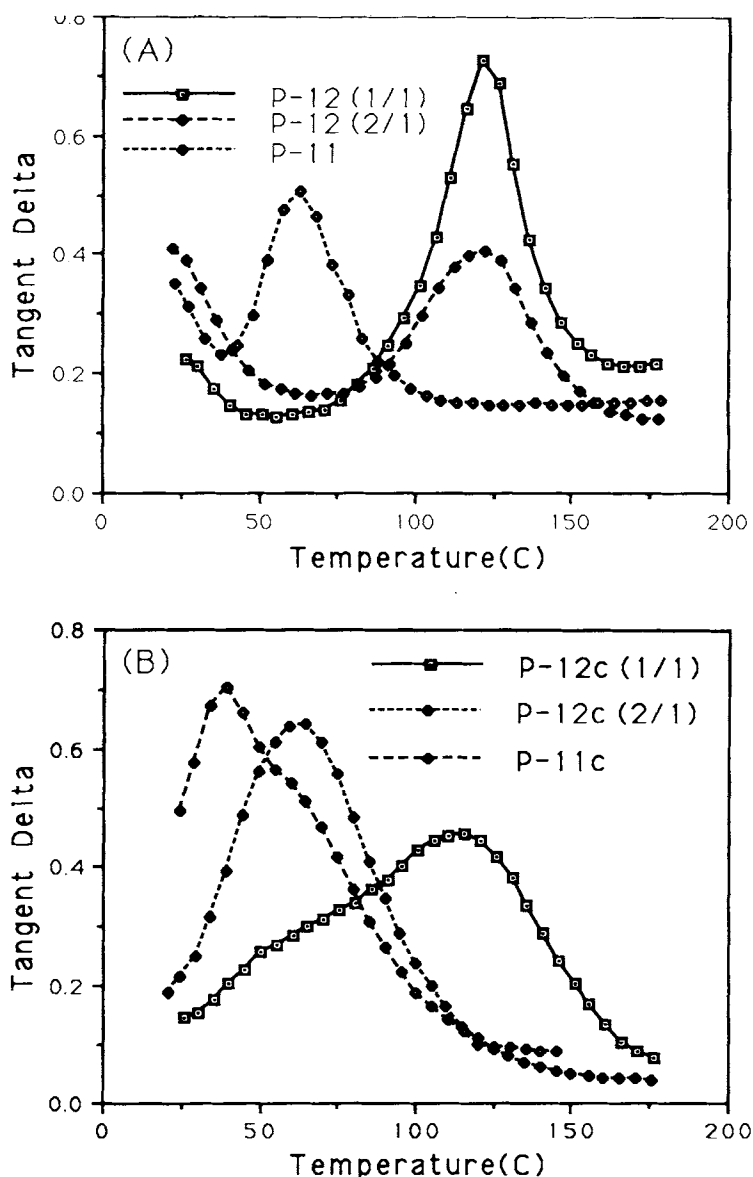


**Figure 7** Plots of tangent delta vs. temperature of three IPNs with urethane phase uncatalyzed (A) and urethane phase catalyzed (B).

then calculated around each resonance peak, using the half-power bandwidth method. A theoretical description of the damping efficiency by this method was mentioned elsewhere.<sup>5,23</sup> In general, there were five frequency peaks observed, that is, five resonance modes, starting from mode I for the lowest resonance frequency to mode V for the high resonance frequency.

Figure 3 illustrates schematically all the five vibration modes measurable in this study. It is noted that large amplitude of mode I can generally be observed for all the tested laminates. Since this large amplitude may result in a loss factor measurement

outside the linear viscoelastic range of the laminated IPN, it is not used for vibration damping analysis throughout this study.

## RESULTS AND DISCUSSION

### Urethane/Acrylate IPNs

#### Damping Properties of IPNs

Figure 4 shows the plots of  $\tan \delta$  vs. temperature for P-11 series ( $U/A = 2/1$ ), along with its two constituents, P-10 (PU) and P-01 (P(MMA/MA)).

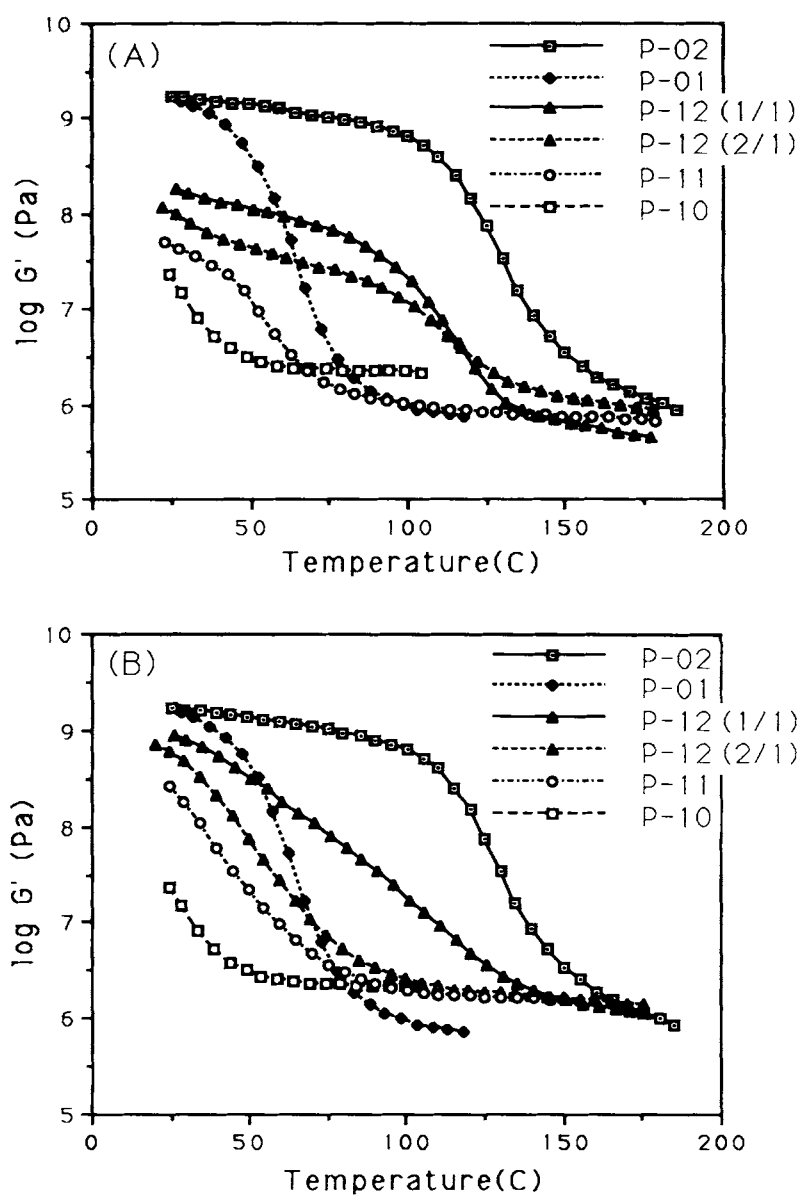


**Figure 8** Plots of storage modulus vs. temperature of three IPNs with urethane phase uncatalyzed (A) and urethane phase catalyzed (B).

All the  $\tan \delta$  peak values and peak temperatures are listed in Table II. The P-10 yields a peak value of  $\tan \delta = 1.3$  at a temperature below  $25^\circ\text{C}$  and the P-01 gives a peak value of  $\tan \delta = 1.7$  at  $75^\circ\text{C}$ . The P-11 (with the urethane phase not catalyzed using T-12) shows two distinguished peaks of *ca.* 0.4 and 0.51, at *ca.*  $25^\circ\text{C}$  and  $63^\circ\text{C}$ ., respectively. Therefore, the peak damping temperatures of the components in an IPN shift inward to some extent, falls between the damping temperatures of its components; its effective damping temperature range is extended with a reduced damping capability. However, this reduced

damping capability still allows an efficient laminate damping, as will be further discussed in another section. This indicates that the two phases in P-11 are only partially interpenetrated. The P-11c (with the urethane phase catalyzed) exhibits only one major damping peak of 0.7 at  $39^\circ\text{C}$ , suggesting that the two phases are well mixed. In other words, the two reactions in the simultaneous semi-IPNs could have a "sequential" nature, depending on the reaction temperature and whether the catalyst is added or not. The P-11c also gives a  $\Delta T = 55^\circ\text{C}$  (temperature range in which tangent delta is greater than 0.4),

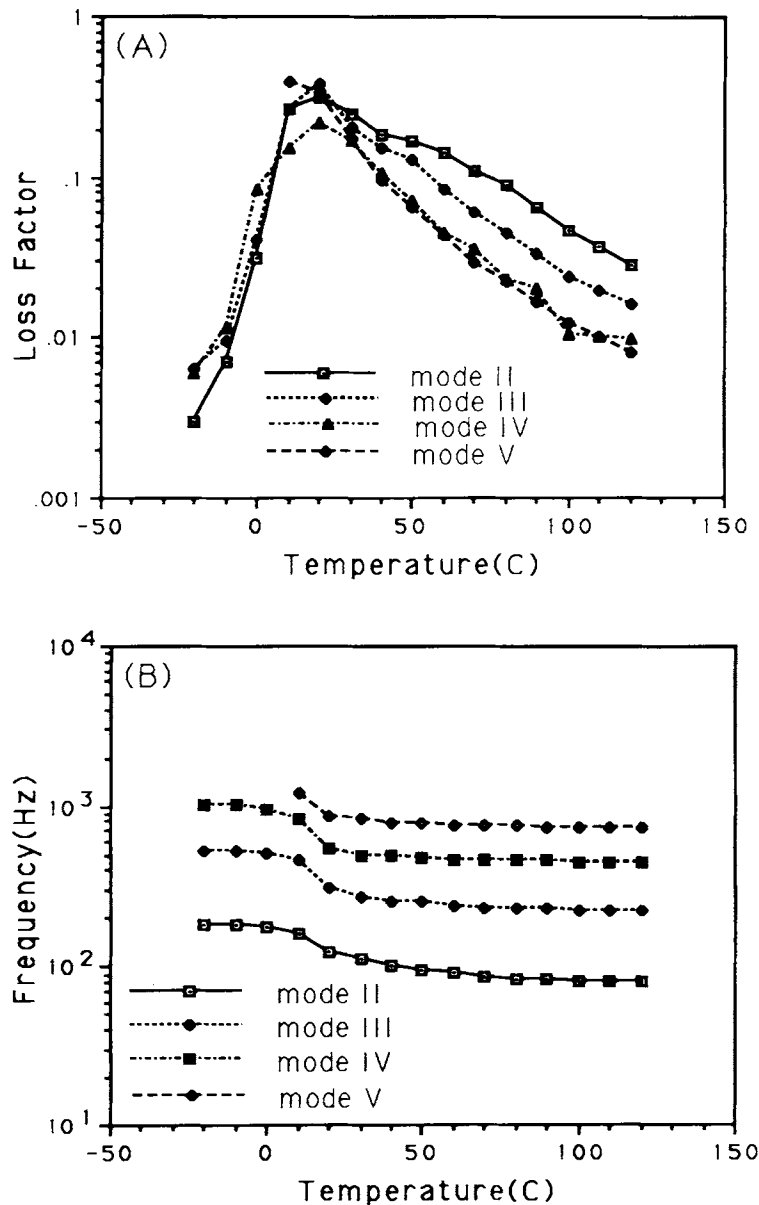


**Figure 9** Temperature dependence of loss factor (A) and temperature dependence of resonance frequency (B) for L-10 laminate at four resonance modes.



far larger than that of P-11. In addition, the damping efficiency of P-11c is better than that of P-11.

When the acrylate phase in IPN is changed from the copolymer MMA/MA to MMA, the damping peak value does not alter much, but the peak temperature increases from 73°C to 135°C (Fig. 5 and Table II), due mainly to the rigid structure of MMA monomer. Figure 5 shows the results of samples P-12 and P-12c (both with U/A = 2/1). Compared to P-12, P-12c exhibits a smoother and broader single damping peak at 64°C with  $\Delta T = 50^\circ\text{C}$ , and a peak value of  $\tan \delta = 0.64$  (Table II). Both  $\Delta T$  and  $\tan \delta$  are greater than the corresponding values of P-12. One can find the same trend in both P-11 series and P-12 series in regard to the damping properties are concerned.

The composition in IPN also affects its damping behavior. Figure 6 shows the results of the P-12 series, in which U/A = 1/1. The P-12 displays a more "separated" phase behavior than P-12c. This can be seen from the distinguished peaks of P-12, with a peak value of 0.22 at *ca.* 25°C and 0.73 at 121°C for the urethane and the acrylate phase, respectively. The P-12c exhibits only a single peak of 0.46 at 116°C. Comparisons of Figures 5 and 6 show that decreasing the catalyzed urethane content in the IPNs decreases the damping capability of IPNs. This may be due to the elastomeric nature of the urethane. Results from Figures 4–6 and from Table II indicate that in general, the IPNs with catalyzed urethane show single, smooth damping curves with peak val-

ues of 0.4–0.7 in a broad temperature range. Note that the temperature depends on the  $\Delta T$  defined.

#### Effect of Network Formation in Urethane Phase

Figure 7 compares the damping properties of three IPNs. In general, the IPNs with uncatalyzed urethane display two separated damping peaks, as shown in Figure 7(A); each is characteristic of the individual components. Increasing the amount of urethane (the P-12 series) does not improve the phase separation. Incorporation of MA into the acrylate phase reduces the glass transition temperature of the acrylate phase, but the two phases in P-11 are still separated. For IPNs with catalyzed urethane, as shown in Figure 7(B), all three IPNs display single, continuously smooth, and broad curves, indicating that phase separation in these IPNs is greatly reduced. This is accomplished by the addition of the catalyst for urethane phase and by lowering the reaction temperature (Table I).

Generally speaking, in the urethane/acrylate IPNs, the mixing-activated urethane phase always polymerizes before the thermally-initiated acrylate phase. The time for the acrylate phase to start the polymerization depends on the amount of the heat involved. The heat may come from external source (i.e., reaction at high temperature) or from the exotherm released from the polymerization of urethane phase. Therefore, the two reactions in an IPN are more or less "sequential." This leads to phase sep-

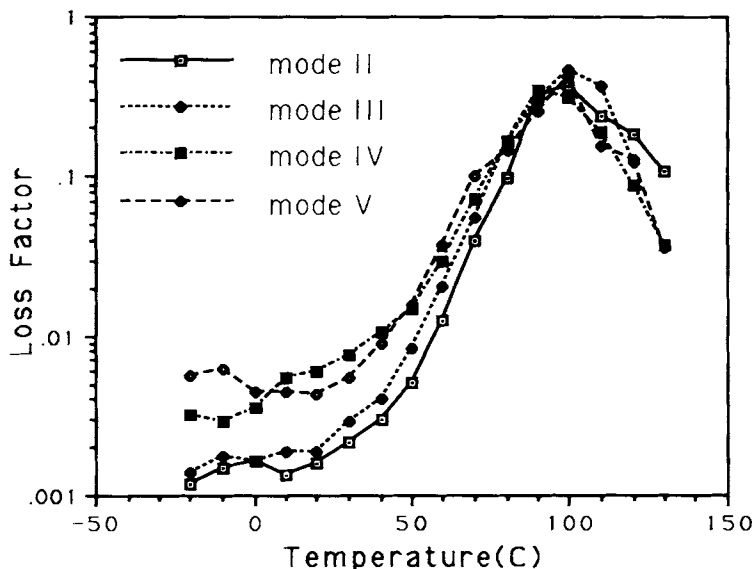


Figure 10 Temperature dependence of loss factor for L-01 laminate at four resonance modes.

aration in most sequential IPNs, as illustrated in Figure 7(A). At a reaction temperature of 80°C, the uncatalyzed urethane polymerizes first and gradually forms the network structure. At the same time, the acrylate phase is still in the monomer or early polymerized stage. This allows the acrylate phase to be phase-separated from the ongoing network formation of the urethane phase.

With the addition of catalyst T-12, the reaction rate of the urethane phase is greatly increased. This can be verified from its relatively short gel time at 35°C as compared with the long gel time for the uncatalyzed urethane reaction at 80°C (i.e., minutes

vs. hours). Therefore, the network is formed in a relatively short period of time in the catalyzed urethane phase. The acrylate monomer is thus "trapped" in the network of the urethane phase. This prevents acrylate monomer phase-separated from the urethane phase when the polymerization of acrylate is eventually completed. Therefore, there is only a single damping curve observed for all three IPNs with catalyzed urethane in Figure 7(B). From the results in Figure 7, it is clear that the effect of catalyst is far greater than the effect of temperature on the reaction kinetics of the urethane phase.

The effect of network formation in the urethane

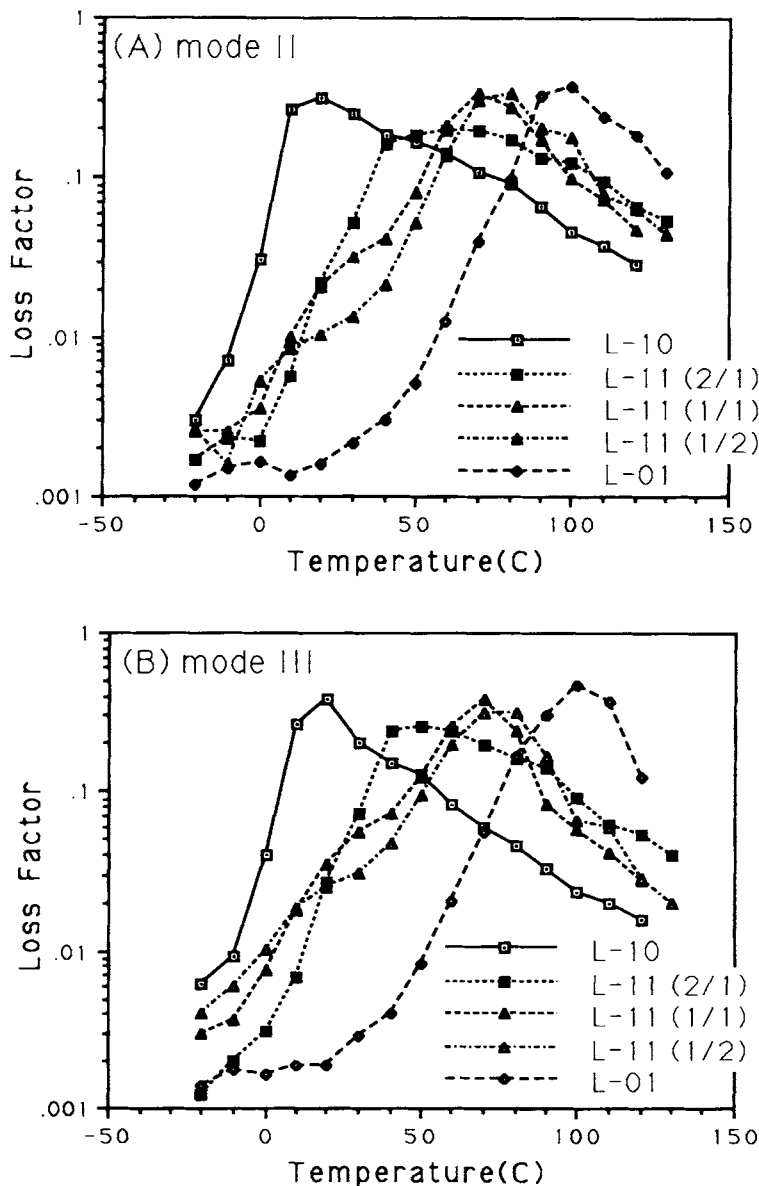


Figure 11 Temperature dependence of loss factor measured at mode II (A), mode III (B), mode IV (C), and mode V (D), illustrating the effect of IPN composition.

phase on the damping property of IPNs can further be understood from Figure 8, where the storage modulus is plotted vs. temperature. The IPNs with uncatalyzed urethane [Fig. 8(A)] show strong peaks of acrylate and urethane phases, respectively. This is not observed in the IPNs with catalyzed urethane, as shown in Figure 8(B). The curves of  $G'$  vs. temperature in Figure 8(B) are smooth compared to Figure 8(A). The rigid network structure, formed in the catalyzed urethane phase, prevents phase separation of acrylate phase from the network structure, resulting in an embedded acrylate phase in the urethane phase. According this reasoning,

there may exist "physical crosslinking" between the urethane phase and the acrylate phase in the IPNs with catalyzed urethane.

### IPN-Laminated Steel Sheets

#### General Description of the IPN-Laminated Steel Sheets

Calculation of the loss factor of the IPN-laminated steel sheet in this study is based on the half-power bandwidth method.<sup>23</sup> The loss factor,  $\eta$ , defined as the ratio of the dissipated energy to the stored energy

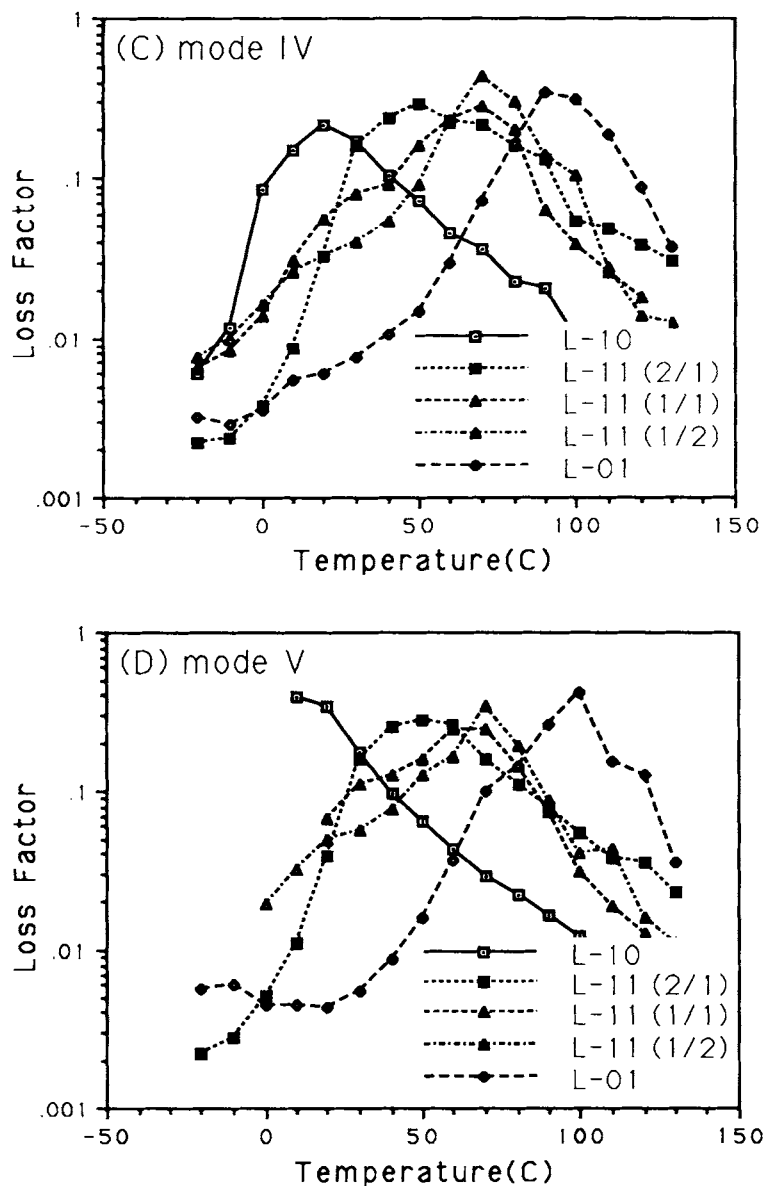


Figure 11 (Continued from the previous page)

per vibration cycle, is a measure of vibration damping efficiency. According to this method,  $\eta$  is given by  $(f_1 - f_2)/fr$ , where  $fr$  is the resonant frequency and  $f_1$  and  $f_2$  the frequencies at the half-power point. In the situation where overlapped peak occurs, the loss factors are calculated by  $\pm 2(fr - f_i)/fr$ ,  $i = 1$  or  $2$ .

Without the addition of the polymeric layer, the loss factor of the neat steel sheet of the same size is usually about  $10^{-4}$  to  $10^{-3}$  at room temperature. Figure 9–11 indicate that the loss factor  $\eta$  of the laminated steel sheet is generally in the range of  $10^{-2}$  to  $10^0$ . The improvement in damping is about 2–3 orders of magnitude. However,  $\eta$  of the laminate is less than the  $\tan \delta$  of its corresponding neat laminated IPN.

Figure 9(A) shows plots of loss factor vs. temperature and frequency vs. temperature for L-10 at four resonance frequencies (starting from mode II at *ca.* 200 Hz to mode V at *ca.* 1600 Hz). For all four modes measured, the loss factor increases with increasing temperature from  $-25^\circ\text{C}$  to *ca.*  $20^\circ\text{C}$ . Above  $20^\circ\text{C}$ ,  $\eta$  decreases with increasing temperature. There exists a maximum loss factor at *ca.*  $T_{\max} = 20^\circ\text{C}$  for all the four modes, for example,  $\eta_{\text{III},\max} = 0.38$  and  $\eta_{\text{IV},\max} = 0.22$  (Table III).

Plots of the temperature dependence of resonance frequency of L-10, as shown in Figure 9(B), reveal that there exists a transition in frequency in each mode as the testing temperature increases. This transition temperature corresponds to the temper-

ature where  $\eta_{\max}$  occurs in Figure 9(A). This illustrates that during the vibration damping test, the applied frequency shifts to a lower value as the laminate reaches its maximum damping. In this sense, one should use the vibration mode in the analysis of laminate damping, instead of the actual applied frequency; the latter is frequently used in the literature data.<sup>2,6,7</sup> Figure 9(B) can be interpreted as temperature dependence of the storage modulus of the constrained polymer layer or, in effect, the apparent storage modulus of the laminate.<sup>11</sup>

Figure 10 is the same plots as Figure 9 for L-01. The same trend as L-10 can generally be observed. One finds that, in general,  $\eta_{\max}$  occurs around 0.4 and  $T_{\max} = 100^\circ\text{C}$ , regardless of the mode type. Also,  $\eta_{\max}$  of L-01 is generally higher than that of L-10, as shown in Table III, consistent with the damping behavior of the neat IPNs shown in Table II. Thus, the L-10 is suitable for low temperature damping and the L-01 is suitable for high temperature damping.

#### Effect of IPN Composition

Figure 11 gives plots of loss factor vs. temperature at four resonance modes of three IPN-laminated steel sheets (L-11 series), along with L-10 and L-01, the laminates with the corresponding IPN components. The composition of each damping layer is summarized in Table III. One can see that generally  $\eta_{\max}$  and  $T_{\max}$  of the L-11 series fall in between those

**Table III** Effect of IPN Composition on Damping Efficiency of the Laminate

U/A	Sample Code				
	L-10 1/0	L-11 2/1	L-11 1/1	L-11 1/2	L-01 0/1
$\eta_{\text{II},\max}$	0.32	0.20	0.34	0.34	0.38
$T_{\text{II},\max}$ ( $^\circ\text{C}$ )	20	65	70	80	100
$\Delta T_{\text{II}}$ ( $^\circ\text{C}$ ) <sup>a</sup>	97	105 <sup>b</sup>	77	78	66 <sup>b</sup>
$\eta_{\text{III},\max}$	0.38	0.26	0.38	0.31	0.47
$T_{\text{III},\max}$ ( $^\circ\text{C}$ )	20	50	70	70	100
$\Delta T_{\text{III}}$ ( $^\circ\text{C}$ ) <sup>a</sup>	77	98	78	72	59 <sup>b</sup>
$\eta_{\text{IV},\max}$	0.22	0.29	0.28	0.44	0.35
$T_{\text{IV},\max}$ ( $^\circ\text{C}$ )	20	50	70	70	90
$\Delta T_{\text{IV}}$ ( $^\circ\text{C}$ ) <sup>a</sup>	63	86	78	70	62
$\eta_{\text{V},\max}$	0.40	0.28	0.25	0.35	0.42
$T_{\text{V},\max}$ ( $^\circ\text{C}$ )	10	50	60	70	100
$\Delta T_{\text{V}}$ ( $^\circ\text{C}$ ) <sup>a</sup>	—	82	80	77	64

<sup>a</sup> All the value of loss factor  $\eta > 0.05$  within  $\Delta T$  range in each mode.

<sup>b</sup> Extrapolated data.

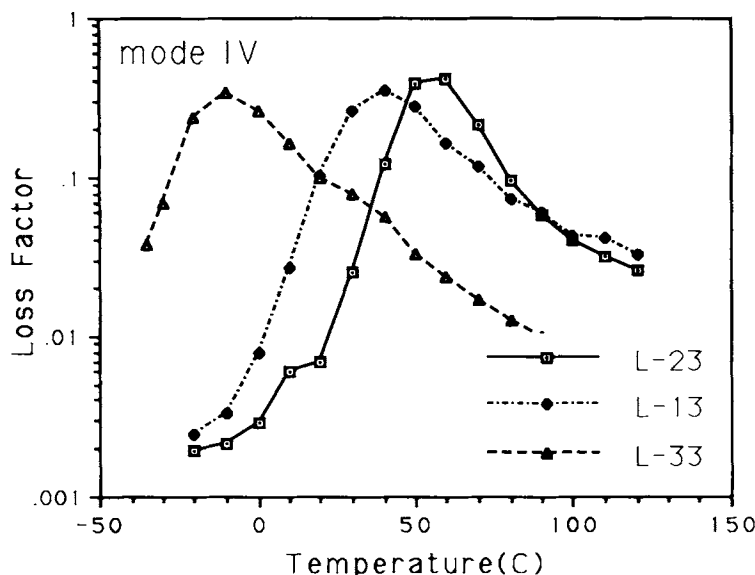


**Figure 12** Temperature dependence of loss factor measured at mode IV, illustrating the effect of urethane composition in IPN.

of L-10 and L-01. This is in general agreement with those observed in the damping behavior of neat IPNs tested using RDA. Of special interest is the broader temperature range of the L-11 series compared to that of L-10 and L-01. This can be observed when one compared the larger  $\Delta T$  of the L-11 series in Table III. The results obviously meet the objective of this study. In addition,  $\eta_{\max}$  and  $T_{\max}$  generally increase with increasing amounts of P(MMA-MA) in IPN. This shows that the laminate with desired loss factor at specified service temperature can be designed through proper selection of the composition in IPN.

#### Effect of Urethane Composition in IPN

In order to examine the effect of urethane composition in IPN on the damping property of the laminate, different types and amounts of polyol, including diol and triol, were employed, as indicated in Table I. While the molar ratio of polyol/MDI (*ca.* 1.04/1) and the theoretical mol wt  $M_c$  of the adjacent crosslinks in PU network (*ca.* 8500) are fixed, the weight ratio of polyol/MDI varies from 1.3/1 (P-23c) to 5.9/1 (P-33c). The constant  $M_c$  was achieved by employing two additional polyols, that is, a diol (A1021, MW = 2000 g/eq) and a triol (A1071, MW = 238 g/eq). Among the three urethane components used, sample P-23c contains the largest amount of the MDI by weight, that is, the largest amount of aromatic moiety in urethane phase.

When these IPNs are laminated with steel sheet, Figure 12 and Table IV indicate that, among the three laminates, L-23 (with the highest content of MDI) exhibits the highest damping temperature  $T_{\max}$ , but only medium  $\Delta T$  range for all four modes. This high  $T_{\max}$  of L-23 is primarily due to the increased amount of MDI in urethane phase, since MDI is more rigid and stiff than the polyol com-

**Table IV** Effect of PU Composition in IPN on Damping Efficiency of the Laminate

	Sample Code		
	L-13	L-23	L-33
$\eta_{II,\max}$	0.25	0.31	0.23
$T_{II,\max}$ (°C)	40	60	-10
$\Delta T_{II}$ (°C) <sup>a</sup>	> 106 <sup>b</sup>	> 84 <sup>b</sup>	77
$\eta_{III,\max}$	0.31	0.41	0.33
$T_{III,\max}$ (°C)	40	60	-10
$\Delta T_{III}$ (°C) <sup>a</sup>	101	81	78
$\eta_{IV,\max}$	0.35	0.42	0.35
$T_{IV,\max}$ (°C)	40	60	-10
$\Delta T_{IV}$ (°C) <sup>a</sup>	83	62	76
$\eta_{V,\max}$	0.31	0.45	0.37
$T_{V,\max}$ (°C)	40	60	-10
$\Delta T_V$ (°C) <sup>a</sup>	68	58	> 60

<sup>a</sup> All the value of loss factor  $\eta > 0.05$  within  $\Delta T$  range in each mode.

<sup>b</sup> Estimated data since  $\eta > 0.05$  within the applied temperature range.

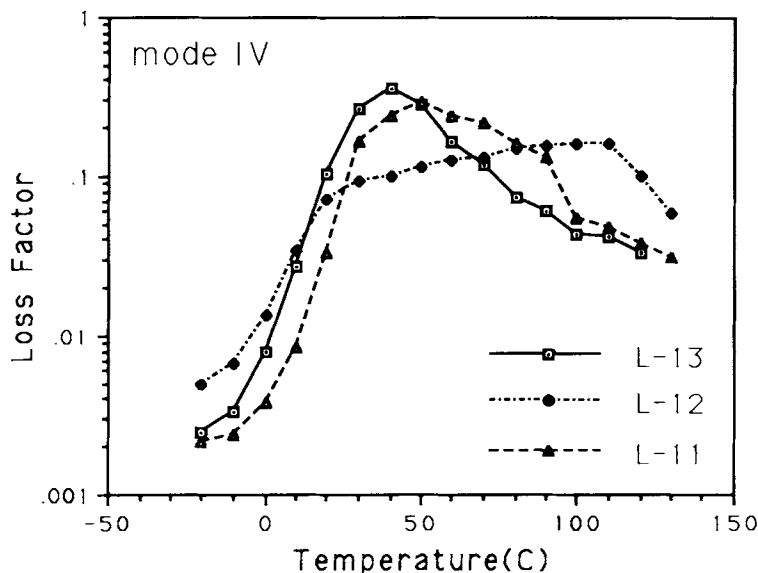


**Figure 13** Temperature dependence of loss factor measured at mode IV, illustrating the effect of acrylate composition in IPN.

ponent because of its aromatic moiety. By the same token, the low  $T_{max}$  of L-33 may result from the increased amount of the “soft” polyol. On the other hand,  $\eta_{max}$  of the three laminates does not show significant change. Technically speaking, a loss factor greater than 0.2 is efficient enough as far as vibration damping of the IPN-based laminate is concerned.

#### Effect of Acrylate Composition in IPN

The composition of the acrylate phase in IPN can also affect the damping properties of the laminate. Figure 13 compares three laminates with different content of acrylate phase in the laminated IPN ( $U/A = 2/1$ ) and Table V summarizes the damping data. Generally speaking, the damping properties ( $\eta_{max}$ ,  $T_{max}$ , and  $\Delta T$ ) of L-13 exhibit strong frequency dependence; as the frequency increases,  $\eta_{max}$  increases, but  $\Delta T$  decreases, while  $T_{max}$  remains insensitive to the applied frequency. On the other hand, L-12 displays damping properties that are independent of the applied frequency. For L-11 with  $\Delta T_g$  located in the middle of neat MMA and MA, it shows a trend similar to those observed in L-13. In addition, increasing the amount of MMA in the acrylate phase results in a decrease in  $\eta_{max}$ ,  $T_{max}$ , and  $\Delta T$ . This suggests that the neat MMA/MA has a strong characteristics of the neat MA.

From the results revealed in Figures 9–13, it can be stated that the damping properties of the IPN-based laminates measured by the frequency spectrum analyzer parallel the damping properties of the

IPNs measured by RDA. These results, together with other damping behavior of the laminates mentioned above, imply that understanding the dynamic mechanical properties of the neat IPN is vital for a

**Table V** Effect of Acrylate Composition in IPN on Damping Efficiency of the Laminate

U/A = 2/1 A $\Delta T_g^a$	Sample Code		
	L-11 MMA/MA	L-12 MMA	L-13 MA
$\eta_{II,max}$	0.20	0.21	0.25
$T_{II,max}$ (°C)	65	110	40
$\Delta T_{II}$ (°C) <sup>b</sup>	105	100 <sup>c</sup>	122
$\eta_{III,max}$	0.26	0.21	0.31
$T_{III,max}$ (°C)	50	110	40
$\Delta T_{III}$ (°C) <sup>a</sup>	98	114 <sup>c</sup>	101
$\eta_{IV,max}$	0.29	0.16	0.35
$T_{IV,max}$ (°C)	50	100	40
$\Delta T_{IV}$ (°C) <sup>b</sup>	86	118	83
$\eta_{V,max}$	0.31	0.14	0.31
$T_{V,max}$ (°C)	40	100 (30) <sup>d</sup>	40
$\Delta T_V$ (°C) <sup>b</sup>	68	116	68

<sup>a</sup> Difference of glass transition temperature of urethane and acrylate components.

<sup>b</sup> All the value of loss factor  $\eta > 0.05$  within  $\Delta T$  range in each mode.

<sup>c</sup> Extrapolated data.

<sup>d</sup> The number in parenthesis indicates that the peak is only a shoulder.

successful design, application, or even prediction, of the IPN-laminated steel sheet.

## CONCLUSIONS

We have demonstrated in this study the vibration damping characteristics of urethane/acrylate IPNs and the IPN-laminated steel sheets. The results are summarized as follows:

1. The dynamic rheological properties of the urethane/acrylate simultaneous semi-IPN were first investigated using RDA. The effect of some IPN variables investigated included the reaction temperature, the amount of catalyst for the urethane phase, the composition of IPN, the composition in acrylate phase, and the composition in the urethane phase.
2. By properly adjusting the above-mentioned variables, mainly the reaction temperature and the amount of catalyst in the urethane phase, the extent of phase separation in IPN could be controlled. This was primarily due to the network structure formed in the catalyzed urethane phase, which prevented the acrylate phase from being separated. The IPNs with catalyzed urethane phase showed single, smooth damping curves with peak values of 0.4–0.7 in a broad temperature range.
3. The above-mentioned IPNs were then laminated between two steel sheets to form IPN-based laminates in order to measure the vibration damping properties of the laminate. These included the effect of IPN composition, the effect of the acrylate composition in IPN, and the effect of the urethane composition in IPN. The results indicated that the IPN-based laminates yielded a maximum loss factor in the range of 0.1–0.5, which was below the maximum  $\tan \delta$  value of neat IPN, but was better than that of the neat steel sheet. In addition, most of the damping properties of the laminates could be derived or predicted from the dynamic mechanical property of the neat IPNs measured by RDA. Therefore, knowing the basic dynamic mechanical property of the neat IPNs is vital for a successful design and application of the IPN-laminated steel sheet.

E-110-06) and by the China Steel Corporation (CSC). The authors wish to acknowledge F. S. Liao and S. I. Chen at CSC for their help in the frequency spectrum analysis.

## REFERENCES

1. J. A. Grates, J. E. Lorenz, D. A. Thomas, and L. H. Sperling, *Modern Paint and Coatings*, **Feb**, 35 (1975).
2. J. A. Grates, D. A. Thomas, E. C. Hickey, and L. H. Sperling, *J. Appl. Polym. Sci.*, **19**, 1731 (1975).
3. N. Pennington, *Modern Metal*, **Feb**, 12 (1987).
4. Y. S. Chen, T. J. Hsu, and S. I. Chen, *Metall. Trans.*, **22A**, 653 (1991).
5. E. E. Ungar, In *Noise and Vibration Control*, L. L. Beranek, Ed., McGraw-Hill, New York, 1979, Chap. 14.
6. A. Jouet and M. Glemet, In *Hot & Cold-Rolled Sheet Steels*, R. Pradhan and G. Ludkovsky, Eds., TMS, Warrendale, PA, 1988, p. 221.
7. N. Chiba, *Nippon Kokan Technical Report*, Fukuyama, Japan, **43**, 50 (1985).
8. E. E. Ungar, *J. Acoust. Soc. Am.*, **34**, 1082 (1962).
9. D. Ross, E. E. Ungar, and E. M. Kerwin, Jr., In *Structural Damping*, J. E. Ruzicka, Ed., ASME, New York, 1959, Sec. 3.
10. E. M. Kerwin, Jr., *J. Acoust. Soc. Am.*, **31**, 952 (1959).
11. F. S. Liao and T. J. Hsu, *J. Appl. Polym. Sci.*, to appear.
12. D. A. Thomas and L. H. Sperling, In *Polymer Blends*, Vol. 2, D. R. Paul and S. Newman, Eds., Academic, New York, 1978, Chap. 11.
13. L. H. Sperling, *Polym. News*, **4**, 206 (1978).
14. K. Kircher, W. Mrotzek, and G. Menges, *Polym. Eng. Sci.*, **24**, 974 (1984).
15. L. H. Sperling, T. W. Chiu, and D. A. Thomas, *J. Appl. Polym. Sci.*, **17**, 2443 (1973).
16. H. Djomo, A. Morin, M. Damyanidu, and G. C. Meyer, *Polymer*, **24**, 65 (1983).
17. G. Allen, M. J. Bowden, D. J. Blundell, G. M. Jeffs, J. Vyvoda, and T. White, *Polymer*, **14**, 604 (1973).
18. R. D. Corsaro and L. H. Sperling, Eds., *Sound and Vibration Damping with Polymers*, ACS Symp. Ser. 424, American Chemical Society, Washington, DC, 1990.
19. D. Klempner, D. Sophiea, B. Suthar, K. C. Frisch, and V. Sendjarevic, *Polym. Mat. Sci. Eng. (Prepr.)*, **65**, 82 (1991).
20. Y. Li, R. Liu, J. Wang, and X. Tang, *Polym. Mat. Sci. Eng. (Prepr.)*, **65**, 134 (1991).
21. R. Y. Ting, R. N. Gapps, and D. Klempner, *Polym. Mat. Sci. Eng. (Prepr.)*, **60**, 654 (1989).
22. J. J. Fay, D. A. Thomas, and L. H. Sperling, *J. Appl. Polym. Sci.*, **43**, 1617 (1991).
23. A. D. Nashif, D. I. G. Jones, and J. P. Henderson, *Vibration Damping*, Wiley, New York, 1985.

This work is sponsored by the National Science Council of the Republic of China (Grant number NCS-80-0405-

Received December 14, 1991

Accepted February 3, 1992